Research Paper

Volume : 3 | Issue : 8 | Aug 2014 • ISSN No 2277 - 8179

Magnetic Non-Potential Parameter in Solar Active Region NOAA 10930

Physics

KEYWORDS : Sun: magnetic fields, sunspots, flares.

Yogita Suthar — Department of Physics, University College of Science, Mohanlal Sukhadia University, Udaipur 313 001, India

S.N.A. Jaaffrey — Department of Physics, PAHER University 313 001, India.

ABSTRACT

We present the evolution of magnetic non potential parameter in AR 10930, during December 9-15, 2006. This AR highly active and produced a large number of flares with two X-class flare. We used 27 high-resolution vector magnetograms obtained with Hinode/SOT-SP. We studied the evolution of spatially averaged signed shear angle (SASSA) and mean weighted shear angle (MWSA) in the N-polarity and S-polarity regions separately. We found the SASSA is same for both polarities. In S-polarity, the MWSA is high compare to N-polarity. SASSA and MWSA show similar trends during the observed period.

INTRODUCTION

The non-potential magnetic field in solar active regions stores the free-energy which is needed to fuel the energetic events like solar flares. The conventional measure of non-potentiality has been the so-called magnetic shear angle (Hagyard et al. 1984, 1990, 1999). This angle measures the difference between the observed and potential field azimuths and has been studied in relation to the flares (Venkatakrishnan et al. 1988). However, angle measures only the deviations of the observed field from potential field vector in the horizontal plane alone. The magnetic energy change following a few flares has been estimated by Schrijver et al. (2008) and Jing et al. (2010). Jing et al. (2010) found that the magnitudes of free magnetic energy were different for the flare-active and the flare-quiet regions. In this paper we study the two non-potential magnetic parameters SASSA and MWSA for AR 10930.

(1) Spatially averaged signed shear angle (SASSA)

The signed shear angle (SSA) represent the deviation of observed transverse vector from potential transverse vector with a positive or a negative sign. We can compute the SSA from the following formula:

$$SSA = tan^{-1}\left(\frac{B_{yo}B_{xp} - B_{yp}B_{xo}}{B_{xo}B_{xp} + B_{yo}B_{yp}}\right)$$

Where B_{xo} ,B_{yo} and B_{xp}, B_{yp} are the observed and potential transverse component s of sunspot magnetic fields, respectively. The specialty averaged values of SSA infer the global non-potentiality of the whole sunspot. The SSA has a similar sign to the photospheric chirality of sunspot (Tiwari et al. 2009).

(2)Mean Weighted Shear Angle (MWSA)

The MWSA represents the changes in magnetic structure and the build-up of the magnetic shear; it was introduced by Wang (1992). The MWSA is given as

$$MWSA = \frac{\sum|B_t|\theta}{\sum|B_t|}$$

Where B_t is the measured transverse field strength and difference between the observed and potential azimuths is given by θ. computation of potential fields were done using longitudinal field as a boundary (Sakurai 1989). The stronger fields have important role for determination of the field structure.

DATA ANALYSIS

We used the vector magnetograms of NOAA 10930 observed on 9 – 15 December 2006 with the Spectro-Polarimeter of Solar Optical Telescope (SOT-SP; Tsuneta et al., 2008; Shimizu et al., 2008; Suematsu et al., 2008; Ichimoto et al., 2008) onboard the Hinode spacecraft (Kosugi et al., 2007). The SOT-SP data were calibrated by the standard SP_PREP.PRO routine developed by Lites and Ichimoto (2013) and are available in the SolarSoft package.

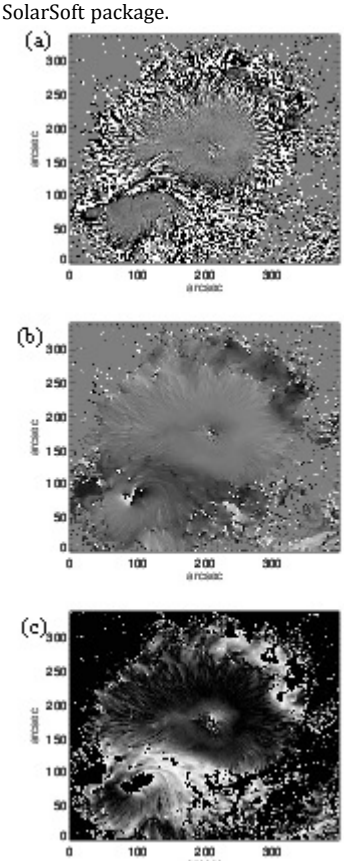

Figure 1: An example of (a) alpha, (b) SSA, and (C) MWSA images of AR 10930 at 17:00 UT on 12 December 2006 obtained with Hinode/SOT-SP.

SOT-SP obtains Stokes profiles of two magnetically sensitive Fe I lines at 630.15 nm and 630.25nm.Photospheric vector magnetograms were derived by Stokes inversion based on the assumption of the Milne–Eddington atmosphere (Skumanich and Lites, 1987; Lites et al., 1993). The 180^0 ambiguity in the vector azimuth was resolved using the minimum energy algorithm by Metcalf (1994).

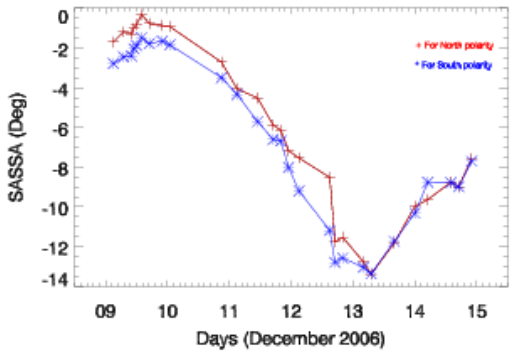

Figure 2: The evolution of SASAA in the S-polarity (blue) and N-polarity (red) regions as a function of time.

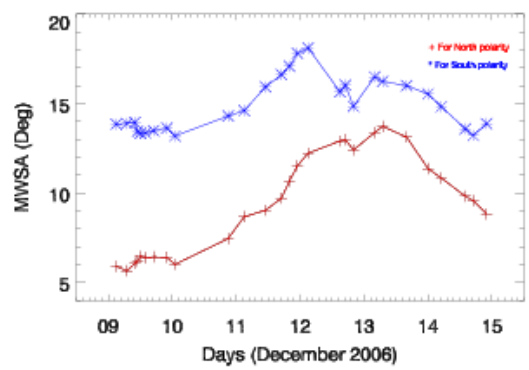

Figure 3: The evolution of MWSA in the S-polarity (blue) and N-polarity (red) regions as a function of time.

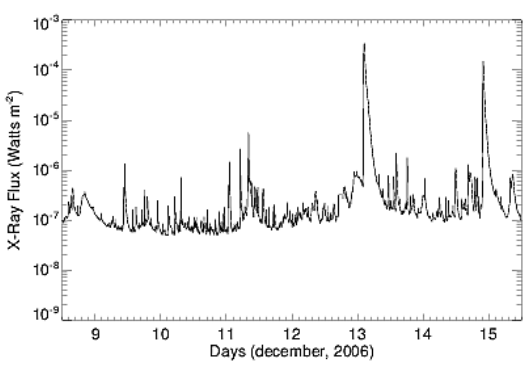

Figure 4: The Temporal evolution of the flare observed by GOES 12 satellites.

The active region NOAA 10930 appeared on the east limb of the Sun on 3 December 2006. Figure 3.1 (left) shows an example of vector magnetograms on 12 December 2006. The small N-polarity sunspot showed an anti-clockwise rotation and emergence of magnetic flux. The large S-polarity sunspot was well developed. The transverse field vectors were highly sheared near the polarity inversion line (PIL) (Zhang, Li, and Song, 2007; Min and Chae, 2009; Ravindra, Venkatakrishnan, and Tiwari, 2011; Ravindra et al., 2011).The continuum intensity image (right) shows that the penumbral fibrils were parallel to the PIL.

We analyzed the signed shear angle (SSA) and Mean weighted shear angle (MWSA) in active region separately for N- and S-polarities. We selected only those pixels whose transverse (B_t) and longitudinal magnetic field (B_z) greater than a certain level. Three vector field components B_x, B_y and B_z are evaluated separately with 1 σ deviations. For transverse field component, we use the resulted deviations in B_x and B_y as a 1σ noise level. We have also used the GOES X-rays plot to find the class of flare.

RESULTS

Figure 2 shows the temporal evolution of SSA for N-polarity (red) and S-polarity (blue) region. Initially, SSA is decreased in both polarities after the flare generation it is increases with similar fashion. Figure 3 shows the temporal evolution of MWSA for N-polarity (red) and S-polarity (blue) region. Before flare generation MWSA increased for both polarities after then it is decreased. All the time MWSA behaves a similar pattern in both polarities. Figure 4 shows GOES 12 X-ray plots in the wavelength range 1-0 Å to 8.0 Å of different X-rays flares. We observed the GOES X-ray peaks show is highly active with two X-class and several M and C class flares during 9-15 December 2006.

DISCUSSION

We have introduced spatially averaged signed shear angle (SASSA) and mean weighted shear angle (MWSA) in active region 10930. Signed shear angle (SSA) provides the sign of twist irrespective of whether the photospheric magnetic field is force-free or not. The sign of SSA is same as the sign of α_g. We conclude that even if the photosphere is non force-free, the sign of global α will empirically give the sign of SASSA and therefore the sign of global twist (chirality) of the sunspots. The flare class, as classified by soft X-ray emission, indicates the maximum amount of X-ray emission and therefore maximum mass of the emitting plasma. MWSA does not show any relation with peak in GOES X-ray plot for different class of flare. The magnetic non potential parameters study in separately N- and S-polarity does not show any effect compare to study of SASSA and MWSA for whole active region (Tiwari, el al. 2010)

Acknowledgements:

Hinode is a Japanese mission developed and launched by ISAS/JAXA, with NAOJ as domestic partner and NASA and STFC (UK) as international partners. It is operated by these agencies in co-operation with ESA and the NSC (Norway).

REFERENCE

1. Hagyard, M. J., Teuber, D., West, E. A., & Smith, J. B. 1984, Sol. Phys., 91,115. | 2. Hagyard, M. J., Venkatakrishnan, P., & Smith, J. B., Jr. 1990, ApJS, 73,159. | 3. Hagyard, M. J., Stark, B.A., & Venkatakrishnan, P. 1999,Sol. Phys., 184,133 | 4. Ichimoto, K., Lites, B., Elmore, D., Suematsu, Y., Tsuneta, S., Katsukawa, Y., 2008, SolarPhys.249, 233. | 5. Jing, J., Tan, C., Yuan, Y., Wang, B., Wiegelmann, T., Xu, Y., & Wang, H. 2010, ApJ, 713,440 | 6. Kosugi, T., Matsuzaki, K., Sakao, T., Shimizu, T., Sone, Y., Tachikawa, S., 2007, SolarPhys.243,3. | 7. Lites, B.W., Elmore, D.F.,Seagraves, P., Skumanich, A.P.:1993, Astrophys. J.418. | 8. Lites, B.W., Ichimoto, K.:2013, Solar Phys.283, 601. | 9. Metcalf, T.R.:1994, Solar Phys.155, 235. | 10. Min, S., Chae, J.: 2009, Solar Phys.258, 203. | 11. Ravindra, B., Venkatakrishnan, P., Tiwari,S.K., Bhattacharyya, R.:2011, Astrophys. J.740, 19. | 12. Ravindra, B., Venkatakrishnan, P., Tiwari, S.K.: 2011, In: Satake, K. (ed.), Advances in Geosciences, Solar Terrestrial (ST) 27, World Scientific, Singapore, 153. | 13. Sakurai, T. 1989, Space Sci. Rev., 51, 11. | 14. Schrijver,C. J., et al. 2008,ApJ, 675,1637. | 15. Shimizu, T., Nagata,S., Tsuneta, S., Tarbell,T., Edwards, C., Shine, R., 2008, Solar Phys.249, 221. | 16. Skumanich, A., Lites, B.W.: 1987, Astrophys. J.322, 473. | 17. Suematsu,Y.,Tsuneta,S.,Ichimoto,K.,Shimizu,T.,Otsubo,M.,Katsukawa,Y.,2008,SolarPhys.249,197. | 18. Tiwari, S. K., Venkatakrishnan, P., & Sankarasubramanian, K.2009b, ApJ, 702, L133. | 19. Tsuneta, S., Ichimoto, K., Katsukawa, Y.,Nagata,S., Otsubo, M., Shimizu, T., 2008, Solar Phys.249, 167.. | 20. Venkatakrishnan, P., Hagyard, M. J., & Hathaway, D. H. 1988, Solar Physics, 115, 125 | 21. Wang, H. 1992, Sol. Phys., 140, 85. | 22. Zhang, J., Li, L., Song, Q.:2007, Astrophys. J.Lett.662, L35. |